ECOSYSTEMS: ECOLOGY AND DYNAMICS, 2023, Vol.7, No. 1, P. 92-114

METHODS FOR STUDYING, MAINTANENCE AND PRESERVING ECOSYSTEMS AND THEIR COMPONENTS

UDC631.4

SATELLITEDATA TO HELP DISTINGUISHCALCAREOUSSOILS IN THE VOLGA-DON IRRIGATION SYSTEM, VOLGOGRAD REGION

© 2023.I.N. Gorokhova*, I.N. Chursin, N.B. Khitrov*, N.K. Kruglyakova*,*****

**V.V. Dokuchaev Soil Science Institute*
Russia, 119017, Moscow, PyzhevskiyPer., 7. E-mail: g-irina14@yandex.ru
***Scientific Geoinformation Center of the Russian Academy of Science*
Russia, 119019, Moscow, p/o 168, Novyy Arbat Str., 11. E-mail: chursin.ivan93@gmail.com
****All-Russian Research Institute of Irrigated Agriculture*
Russia, 400002, Volgograd, Timiryazeva Str., 9. E-mail: kruglyakova02032013@yandex.ru

Received December 16, 2022. Revised February 01, 2023. Accepted February 02, 2023.

In this study we substantiate the importance of identification of the areas with calcareous soils on the key plot of the "Oroshayemaya" experimental station that belongs to the Volga-Don irrigation system, Volgograd Region, using high-resolution satellite data (Pleiades). Carbonates in soils have both a positive and a negative impact; therefore, it is important to identify such soils. We identified calcareous areas on the satellite images, judging by the spots of various degrees of soil effervescence on the surface, caused by HC1 solution, which, in its turn, was detected via the contact method in the cultivated fields. After that we determined a relationship between the spectral brightness of soil effervescence in different channels of the satellite image and its degree. In order to do this, we took a sample of pixels from the images that corresponded to the patches of surface effervescence in the terrain that was previously used in the Random Forest algorithm to select classes in the image. The results showed that identification of the areas with surface layer of calcareous soils (soil effervescence), using satellite data, will be the most optimal if the field research and the survey data took place during the dry season of the year, i.e. from May to July.

For image processing the images of open fields should be used, while the undeveloped ones should be ignored. It is also necessary to exclude patches of meadow and meadow-chestnut soils from the sample, since they are usually located in depressions and can interfere with calculations due to the carbonates that flow in from the side. It is best to allocate the areas of calcareous soils within a single field or within a group of fields with similar brightness level; different brightness levels indicate different types of land use, such as dry farming and irrigated fields. Such a differentiated approach allows the precision of soils classification on the satellite image reach 0.75-0.90, based on the degree of their effervescence (no effervescence, weak, average, strong). However, when the entire key plot is processed, only the soils with "strong effervescence" or "no effervescence" can be identified with the precision of 0.7. The novelty of our work results lies in the substantiation of the possibility to reliably identify (while following all the requirements) calcareous soils on the ground surface by using high-resolution satellite data together with field survey data.

Keywords: calcareous soils, soil effervescence, degree of soil effervescence, open surface, satellite imagery, spectral brightness, classification precision, Volgograd Region.
DOI: 10.24412/2542-2006-2023-1-92-114
EDN: CXMSUO

Land resources are the main natural resource of the Volgograd Region. Among the federal subjects of the Russian Federation, it is the third one, after the Altai Krai and the Orenburg Region, with the largest area of agricultural land (8.7 million ha). The Volgograd Region is a well-developed territory, and so the further expanse of agricultural lands is practically impossible there (Volgograd region …, 2011). The main types of agricultural land appeared there in the early 1960s, after the development of virgin and fallow lands and the widespread irrigation, the latter being

especially extensive in the dry steppe zone.

In pre-revolutionary Russia, the geography of steppe soils was reconsidered in the works of such Russian researchers, as N.A. Dimo and B.A. Keller (1907), G.N. Vysotsky (1915), who showed the diversity of vegetation and soil covers, as well as the relationship between the soils and the microrelief. However, the main patterns of the natural state of soils in the dry steppe under the virgin soil conditions, as well as at the initial stages of their active agricultural development, were established by USSR researchers (Antipov-Karataev, 1953; Ivanova, 1928; Kovda, 1937; Rode, 1947; Ivanova and Friedland, 1954). Long-term studies were summarized by specialists from various organizations in the book "Soils of the Volgograd Region" by E.T. Degtyareva and A.N. Zhulidova (1970).

From the 1960s to the present days, more methods of soils study have been introduced to the classical ones, including remote sensing based on aerial and satellite imagery with high-resolution satellite data (Gorokhova et al., 2018; Wang F. et al., 2020; Wang J. et al., 2019), data from unmanned aerial vehicles (Tian et al., 2020), as well as the use of various remotely determined parameters, such as the indices of vegetation, salinity and soil moisture, surface temperature, topography. In addition, various models for calculating and soil mapping are used, the most popular being Random Forest (RF), multiple linear regression (MLR), support vector machine (SVM), and artificial neural networks (ANN; Gorokhova et al., 2021; Tian et al., 2020; Wang F. et al., 2020; Zarea et al., 2020). However, there is no algorithm that works perfectly for the entire data set; therefore, one algorithm that suits specific goals of the research in the study area must be chosen every time. This is why the interpretation of remote data requires a mandatory and thorough study of the area with the help of field work and laboratory analyzes of soil samples (Gorokhova et al., 2021; Wang F. et al., 2020).

In the 1950s and 1960s large irrigation systems were built in the Volgograd Region. However, by the 1990s improper exploitation of irrigated lands raised the groundwater level, causing flooding and creating niduses of secondary salinization, as well as soils alkalization. As a result, most irrigated lands were abandoned and turned into perennial fallows, while the rest of the lands were repurposed for dry farming, and in the remaining areas the type of irrigation was switched, mainly from the surface irrigation to sprinkling or drip irrigation. Then, during 1990-2010, the groundwater level decreased down to 5 m, and the partial desalination and alkalization began in the secondarily saline soils of the irrigated lands. Due to thee phenomena, the accumulation of carbonates in the surface horizon was especially pronounced. Since the presence of carbonates has a significant effect (both positive and negative) on soil properties, it is an important task to detect and identify calcareous spots in the irrigated fields.

The aim of our article is to use satellite imagery in order to determine carbonate spots of surface soil effervescence in the fields of the "Oroshayemyy" key plot.

Materials and Methods

The object of our study is the Volga-Don irrigation system, located in the dry steppe zone of the Volgograd Region, to the west of Volgograd, in the south of the Volga Upland that gently descends to the Volga-Don Canal. We conducted our research in the territory of the federal state budgetary institution "Experimental Station 'Oroshayemaya'" (hereinafter referred to as the experimental station "Oroshayemaya"), located in the center of the Volga-Don irrigation system (Fig. 1).

The experimental station "Oroshayemaya" was built in the south of the Volga Upland which is stretched along the right bank of the Volga River. Its territory is a plateau, dissected by numerous river valleys, ravines and gullies. It is slightly convex and gradually going down to the edges of the valleys. To the south of Volgogradit merges into the Yergeni Upland. Its relief has formed under the intense manifestation of the latest tectonic uplifts and erosions.

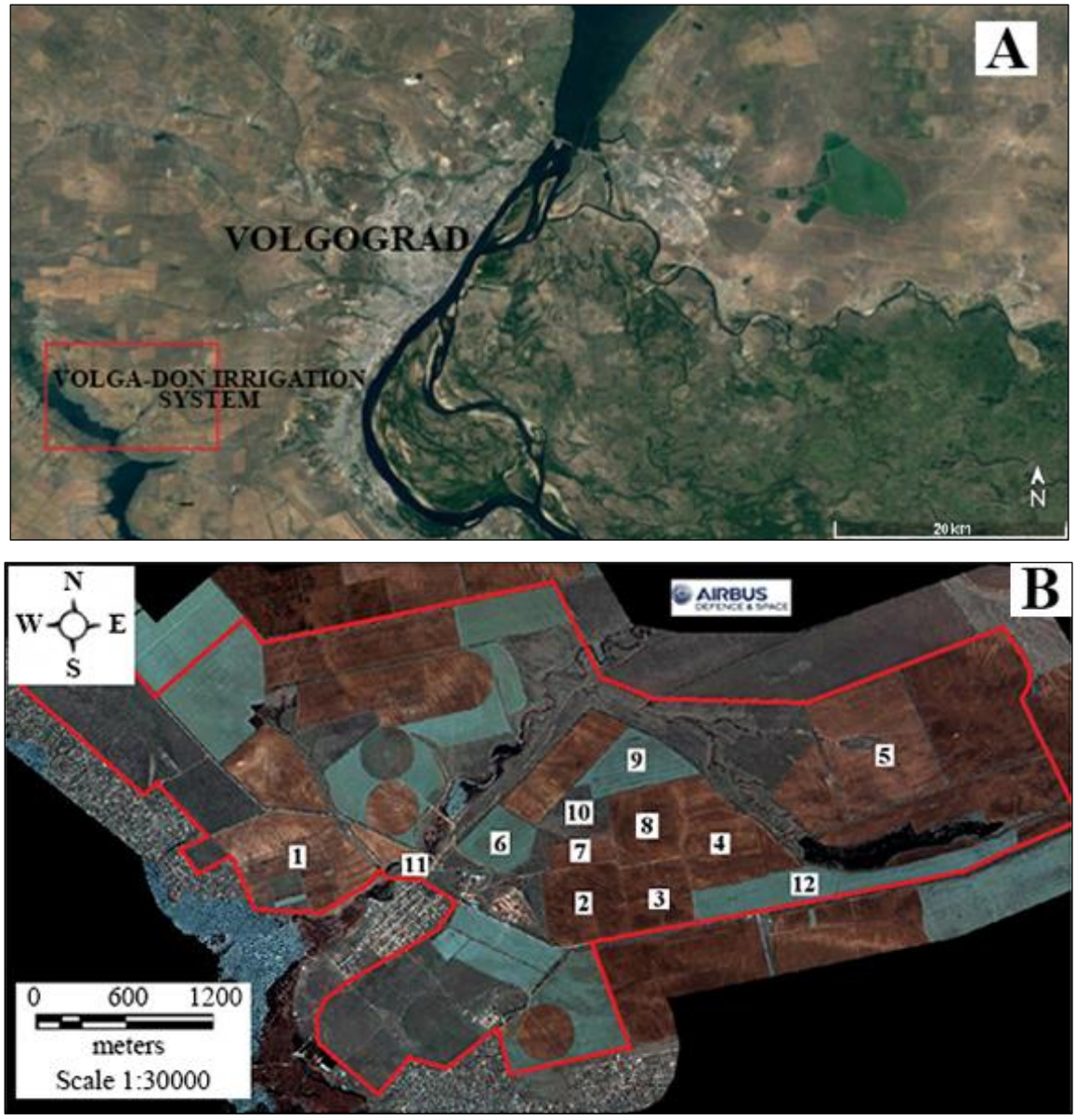

Fig. 1. A – Volga-Don irrigation system on a Google.Earth satellite image, 25/05/2021, B – territory and fields of the key plot of the "Oroshayemaya" experimental station in the Volgograd Region, taken from the Pleiades satellite, 25/04/2020.

During the Pliocene this part of the Volga Upland was completely covered by the Yergeni deposits, formed by sands with layers and lenses of clay and sandstone, which were denuded at the end of the epoch and in the Quaternary. A cover of Yergeni sediments as deep as 30-40 m, as well as the features of a Pliocene accumulation is currently preserved there. The areas near the watersheds are composed of Yergeni sands, covered by the red-brown Scythian clays of 3-50-meter depth, with undetermined genesis and age (Upper Neogene, Lower Quaternary), as well as a mass of Quaternary loess-like loams reaching down to 50-70 m in some places, usually, with low mineralization and sodium bicarbonate composition (Volgograd region ..., 2011).

The south of the Volga Upland is a subzone of chestnut soils. There, the soil-forming rocks are very diverse, giving the soils profile and properties a variable structure. The main forming rocks are Yergeni sands, loess-like loams, and sometimes red-brown Scythian clays. The soil cover is

represented by various combinations, such as chestnut non-solonetzic soils in the areas near the watersheds; solonetzic complexes with different proportions of chestnut soils and solonetzes; automorphic semihydromorphic and hydromorphic solonetzes; combinations and patches of meadow-chestnut and meadow soils of various salinity and alkalinity; alluvial soils of the river valleys (Degtyareva, Zhulidova, 1970; Zinchenko et al., 2020).

The experimental station takes water for irrigation from the Bereslavsky and Varvarovsky reservoirs that belong to the Volga-Don Canal named after V.I. Lenin (Reservoirs, ponds and lakes ..., 2020). In the sub-arid conditions high consumption of water due to surface evaporation from the water bodies increases water mineralization (Table 1).

Table 1. Chemical composition of the water from the Bereslavsky (1) and Varvarovsky (2) irrigation reservoirs of the Volga-Don Canal, August 2020.

Water reservoir	pH	HCO_3^-	Cl^-	SO_4^{2-}	Ca^{2+}	Mg^{2+}	Na^+	K^+	M, g/L	*SAR*
		mmol(equiv)/L								
1	8.1	3.6	4.4	6.1	4.8	2.5	7.0	0.11	0.95	3.7
2	8.2	2.7	3.9	5.9	5.0	1.8	6.0	0.12	0.84	3.2

Notes to Table 1: M–water mineralization, *SAR*– sodium adsorption ratio that estimates the alkalization risks, $SAR = \frac{C_{Na}}{\sqrt{\frac{(C_{Ca}+C_{Mg})}{2}}}$, where C_{Na}, C_{Ca}, C_{Mg} are a concentration of Na^+, Ca^{2+} and Mg^{2+} iones, mmol(equiv)/L (Richards, 1954).

The predicted content of exchangeable sodium in the irrigated soils, when the water values are as shown in Table 1, but the concentration of water in the soils is not taken into account, is 5.1 and 4.4% of the cation exchange capacity. In reality, a constant irrigation carried out with low-salt reservoir water that has an excessive concentration of sodium ions enhances the process of secondary soil alkalization, which is more than 5% of the cation exchange capacity, when estimated by the content of exchangeable sodium (Fig. 2).

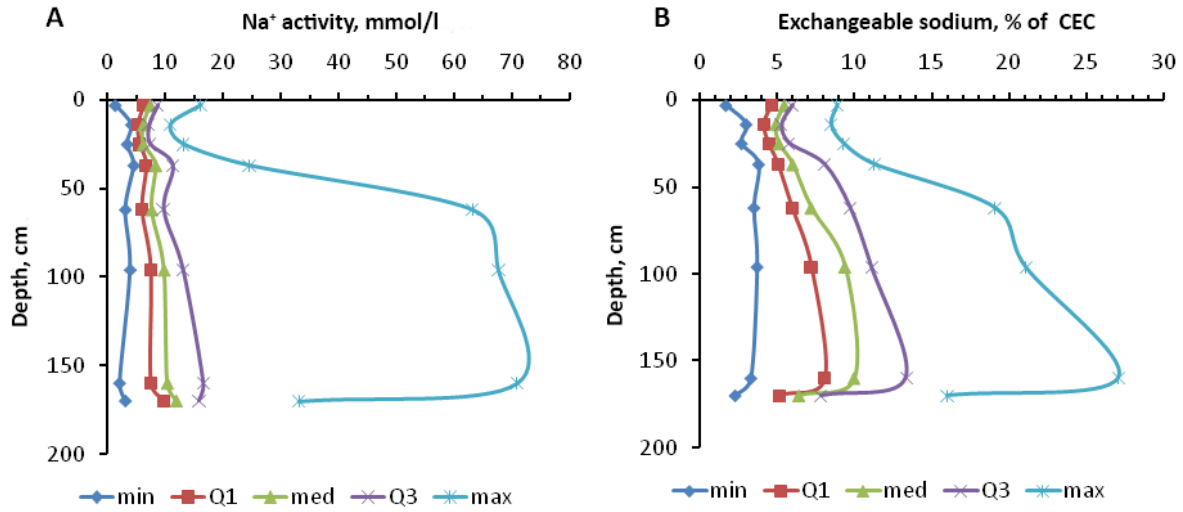

Fig. 2. Distribution of non-parametric statistical indices in a soil profile: A – activity of Na^+ ions in pastes with a moisture content of 40% (wt.), B – exchangeable sodium. *Legend:* min – minimum, med – median, max – maximum, Q1 and Q3 – lower and upper quartiles; sample size is 40 profiles.

The quality of irrigation water and sprinklers, combined with the mesorelief of the territory, have predetermined the development of such degradation processes in the irrigated soils as secondary alkalization, formation of anthropogenic lumpiness, irrigation erosion, and carbonate enrichment in the surface horizons. However, secondary alkalization, while stimulating the development of irrigational erosion, leads to periodic plowing of the lower carbonate horizons and forming of extra patchiness in the field due to carbonates in its top layer. All of this leads to an inhomogeneous pattern of the soil surface that is seen on the satellite images.

Main Theses of the Methodology

The studied key area is the "Oroshayemaya" experimental station, which consists of several fields. We studied a total of 12 fields (Fig. 1B, fields No. 1-12), where the main soil profiles, with description and soil samples, and the test plots for soil effervescence were set along the catena. During our study some of the fields were irrigated (No. 2, 3, 8, 12, southern part of field No. 1), some were repurposed for dry farming after irrigation (No. 4, 5, 6, 9, middle part of field No. 1), and some were always used for dry farming (No. 10, northern part of field No. 1).

Carbonate content is an important feature of soils. Those that have 1% and more alkaline earth carbonates in any of their horizons are classified as carbonate-containing soils (Classification ..., 2004). Calcium carbonate in soils strongly affects many of their properties, such as alkalinity, composition of exchangeable cations, and physical properties. It is possible to detect and roughly determine the content of carbonates out in the field when carbon dioxide is being released after soil's interaction with a 10% solution of HC1, the process known assoil effervescence (Guidelines ..., 2006; Guide ..., 2012). While looking for carbonates in the field, we assessed the degree of effervescence according to the following gradation: absence (no effervescence), weak, average, strong, and local. The routes of testing plots for surface soil effervescence are shown in Figure 3.

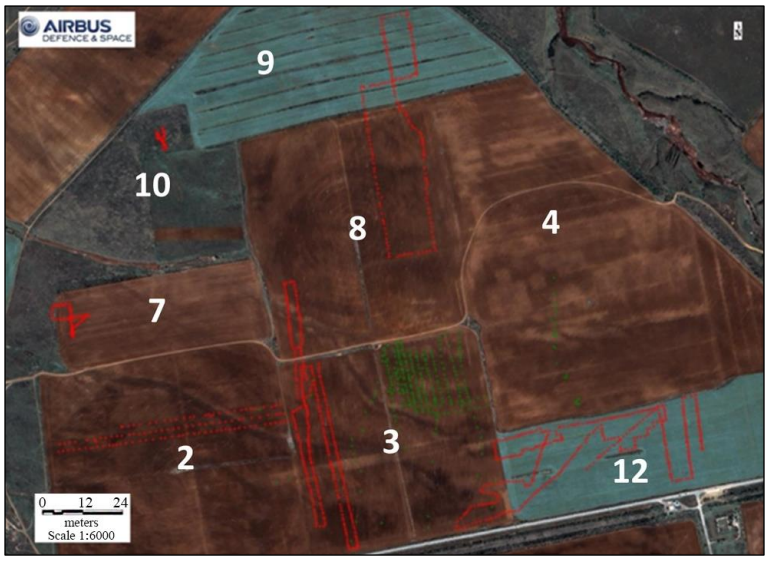

Fig. 3. Routes where the surface soil effervescence was determined on the cultivated fields, using the 10% solution of HC1,in the territory of the "Oroshayemaya" experimental station, marked on a fragment of the Pleiades satellite image, 25/042020.

Then, in order to understand whether the degree of effervescence changes depending on its spectral brightness, we established a relationship between the brightness in different channels (B1-B4) of the Pleiades satellite image, taken on 25/04/2020, by the spots with soil effervescence, and the surface effervescence degree. For that we took a sample of pixels from the images that corresponded to the sampling plots in the open areas. This sample became a basis for a table shown in Figure 4.

	B1	B2	B3	B4	Class
2	747.0	1026.0	1417.0	2075.0	1
3	777.0	1027.0	1418.0	2108.0	2
4	858.0	1154.0	1594.0	2361.0	2
5	787.0	1032.0	1435.0	2069.0	2
6	811.0	1088.0	1471.0	2131.0	2
7	864.0	1194.0	1631.0	2406.0	2
8	825.0	1099.0	1470.0	2187.0	3
9	865.0	1164.0	1604.0	2402.0	3
10	816.0	1092.0	1511.0	2168.0	2
11	854.0	1168.0	1548.0	2468.0	2
12	801.0	1095.0	1506.0	2242.0	5
13	844.0	1099.0	1479.0	2203.0	4
14	816.0	1102.0	1492.0	2218.0	3
15	779.0	998.0	1285.0	1911.0	1
16	824.0	1059.0	1365.0	2015.0	5
17	781.0	1015.0	1291.0	1905.0	4
18	758.0	1010.0	1362.0	2019.0	5
19	777.0	1017.0	1305.0	1918.0	1
20	813.0	1035.0	1329.0	1985.0	5
21	737.0	930.0	1213.0	1782.0	5
22	751.0	963.0	1235.0	1834.0	4
23	809.0	1050.0	1379.0	2021.0	4

Fig. 4. An example of a table of brightness of the B1-B4 channels and soil effervescence degree at the sampling plots from the Pleiades satellite image, taken on 25/04/2020. *Legend:* 1-5 in the "Class" column – the degree of soil effervescence, where 1 means no effervescence, 2 – weak, 3 – average, 4 – strong, 5 – local.

In B1-B4 columns the brightness of the pixels is given in the Blue, Green, Red and NIR channels; the Class column indicates the degree of effervescence at the corresponding plot.

Then we made scatterplots of pixel brightness for all channels.

Results and Discussion

For a preliminary assessment of the possible relationship between the effervescence degree and the pixel values from our sample, we built two-dimensional scatterplots, with the pixel values in each of the channels shown along the axes (columns B1-B4). A total of 6 scatterplots were built for each combination of channels: B1-B2, B1-B3, B1-B4, B2-B3, B2-B4, B3-B4. If individual classes in such scatterplots, highlighted in color, are grouped together instead of mixing with the others, then the sample has a good linear distinguishability. In our case, however, all classes were mostly mixed, meaning a poor distinguishability by the effervescence degree in all 4 channels (Fig. 4).

We used the Random Forest algorithm to statistically confirm poor or acceptable pixel distinguishability and the possibility to distinguish classes for all channels. For the algorithm training, 1/3 of the sample was left for testing and therefore was not used in training. The resulting statistical model was evaluated according to the following parameters.

1. An *error matrix* is usually used to classify an imbalanced data set. It compares the actual values with the ones predicted by the machine-learning model. In the error matrix the diagonal shows those pixels that are correctly assigned to the distinguished classes according to the degree of soil effervescence, where 1 means no effervescence, 2 – weak effervescence, 3 – average, 4 – strong, 5 – local, i.e. where the predicted values correspond to the actual ones. Anything above those is a false positive result, while anything below is a false negative result. The matrix in Figure 5 demonstrates that classes 2, 3 and 5 from the data set for the key plot with an open soil surface are not quite distinguished, while only half of the cases are correctly identified for the classes 1 and 4 (Fig. 6, Table 2).

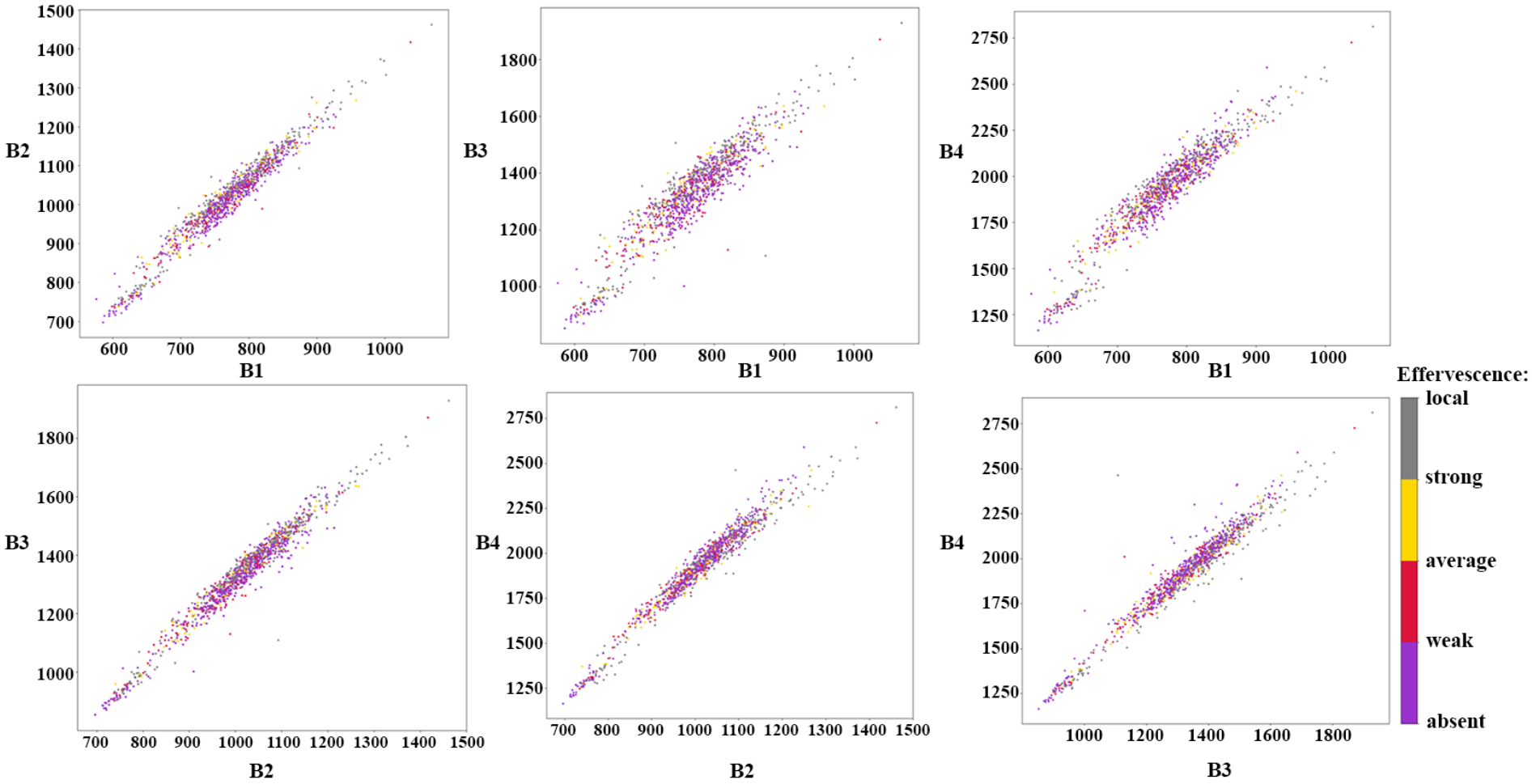

Fig. 5. Scatterplots of pixel brightness and soil effervescence degree (highlighted in color) at the sampling plots of the key area with an open soil surface in the Blue (B1), Green (B2), Red (B3) and NIR (B4) channels, based on a Pleiades satellite image taken on25/04/2020.

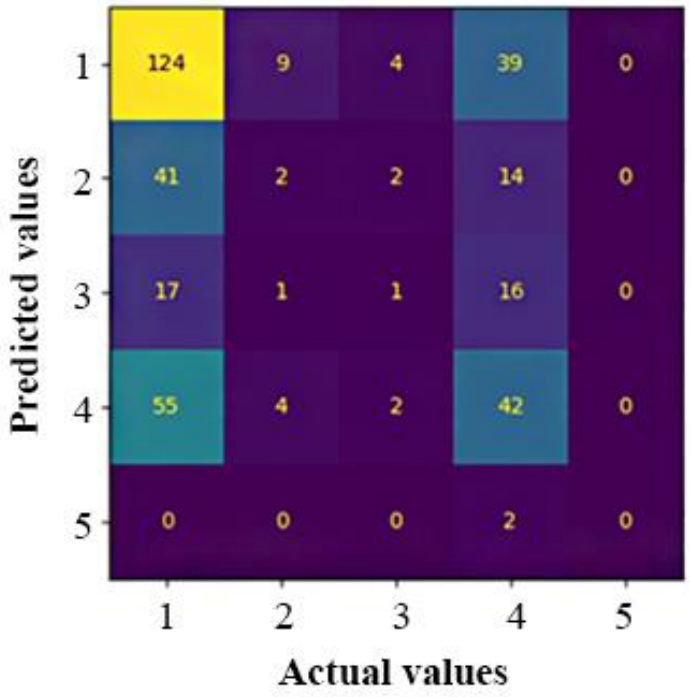

Fig. 6. Error matrix of the classified image of the key area for surface soil effervescence degree, based on the Pleiades satellite image, 25/04/2020. *Legend:* 1 – no effervescence, 2 – weak effervescence, 3 –average, 4 – strong, 5 – local.

Table 2. Statistical indices of the classification of the key area image, according to the degree of surface soil effervescence, using the Random Forest and the Pleiades satellite image, 25/04/2020.

Indices (metrics)	Precision	Recall	F-score	Sample
1 – no effervescence	0.52	0.7	0.6	176
2 – weak effervescence	0.12	0.03	0.05	59
3 – average effervescence	0.11	0.03	0.05	35
4 – strong effervescence	0.37	0.41	0.39	103
5 – local effervescence	0	0	0	2
Percentage of correct answers	–	–	0.58	379
Macro-averaging	0.58	0.58	0.58	379
Weighted arithmetic mean	0.58	0.58	0.58	379

2. *Cross-validation* is a method of model evaluation. For that some partitions from the original sample are divided into two subsamples, the training one and the control one. For each partition the training subsample is used to set a certain algorithm, and then its average error is estimated using the objects from the control subsample. A cross-validation estimation is the mean value of the error in the control subsamples, calculated for all partitions. The results of cross-validation applied to the data set for the entire key plot, where the sample was divided into 5 parts, showed the precision of this classification as follows: 0.430, 0.401, 0.441, 0.498, 0.507.

3. *Precision* is the percentage of correct answers given by the model within one class relative to all objects assigned to the said class.

4. *Recall* is the percentage of true positive classifications. It shows what percentage of objects of the positive class was predicted correctly.

5. *F-score*. It is impossible to actually achieve both maximum precision and recall, therefore, a

certain balance should be found, a parameter to combine information about the precision and recall of the algorithm. This parameter is the F-score, independent from the ratio of classes, and therefore applicable when the samples are unbalanced. F-score is the harmonic mean between precision and recall; if they tend to zero, it tends to zero as well.

Macro-averaging and weighted arithmetic average characterize the entire data set.

Classification indices (metrics) of the pixels sample in the image that correspond to the sampling plots with soil effervescence in the key area are listed in Table 2.

These calculations show that the precision of classification by the degree of surface soil effervescence in the image of our key area does not exceed 0.58, therefore there is no sense to use this classified image.

In the next approach a more balanced classification of the sample by the generalized characteristic of soil effervescence (present/absent) is used. In the Figure 7 the two-dimensional scatterplots are shown that allow us evaluate the possibility of distinguishing classes for all channels.

Figure 7 shows that points from different classes are mixed together, which indicates that the sample differentiates poorly by 2 classes (present/absent) in all channels in terms of the surface effervescence degree.

The error matrix and statistical indicators (metrics) in Figure 8 and Table 3 show that even with a more balanced sample (192/187 pixels) the precision of image classification into 2 classes by surface effervescence also did not exceed 0.58.

The further sample processing was carried out differently. The brightness values of meadowish- and meadow-chestnut soils were removed from it, which may have surface effervescence due to alluvium of carbonate material from neighboring areas, but which have a darker tone in the image due to higher humus content, interfering with the calculations.

Values with local, weak and average effervescence were excluded, while those with strong and no effervescence were considered. Then we determined the spectral brightness of the points of another image, the RGB one obtained from Yandex services (Pleiades, 28/06/2020) for a warm and dry period of July 2020. The result is the error matrix and statistical parameters which can be seen in Figure 9 and Table 4.

The precision of 2-class classification (strong effervescence/no effervescence) was 0.7. Therefore, it is better to use an image taken during a drier period to prevent soil moisture from masking the pixels brightness and to exclude the meadowish- and meadow-chestnut soils from the sample as the darker ones in the image, and use for the further analysis only the values from the points with strong effervescence and without it.

While analyzing the images, we noticed that the fields with open surface had different brightness ranges in the 4 channels. So, we assumed that the fields in the study area could be divided into groups with similar ranges and classified by groups or by individual fields within each group. When partitioned like that, the classification precision of surface effervescence should improve significantly.

For this approach we used a Pleiades image taken on 25/04/2020, and excluded fields both with the vegetating crops and located outside the range of agricultural development. Next, we made scatterplots (Fig. 10), with the colors showing the same brightness ranges of the fields (A) and the different ones (B). Based on these scatterplots, we identified the following groups of fields with similar brightness: 1) fields No. 1, 5; 2) fields No. 2, 3, 8; 3) fields No. 4 and 7. We excluded fields No. 6, 9 and 12, because at that moment they had vegetating crops, field No. 10 because it was a fallow, and field No. 11 because it was a gully valley (Fig. 1).

We have created a program for automated interpretation of images to classify soils with open surface according to the degree of their effervescence. The algorithm of this program is shown in Figure 11. The space image processing was performed as described further below.

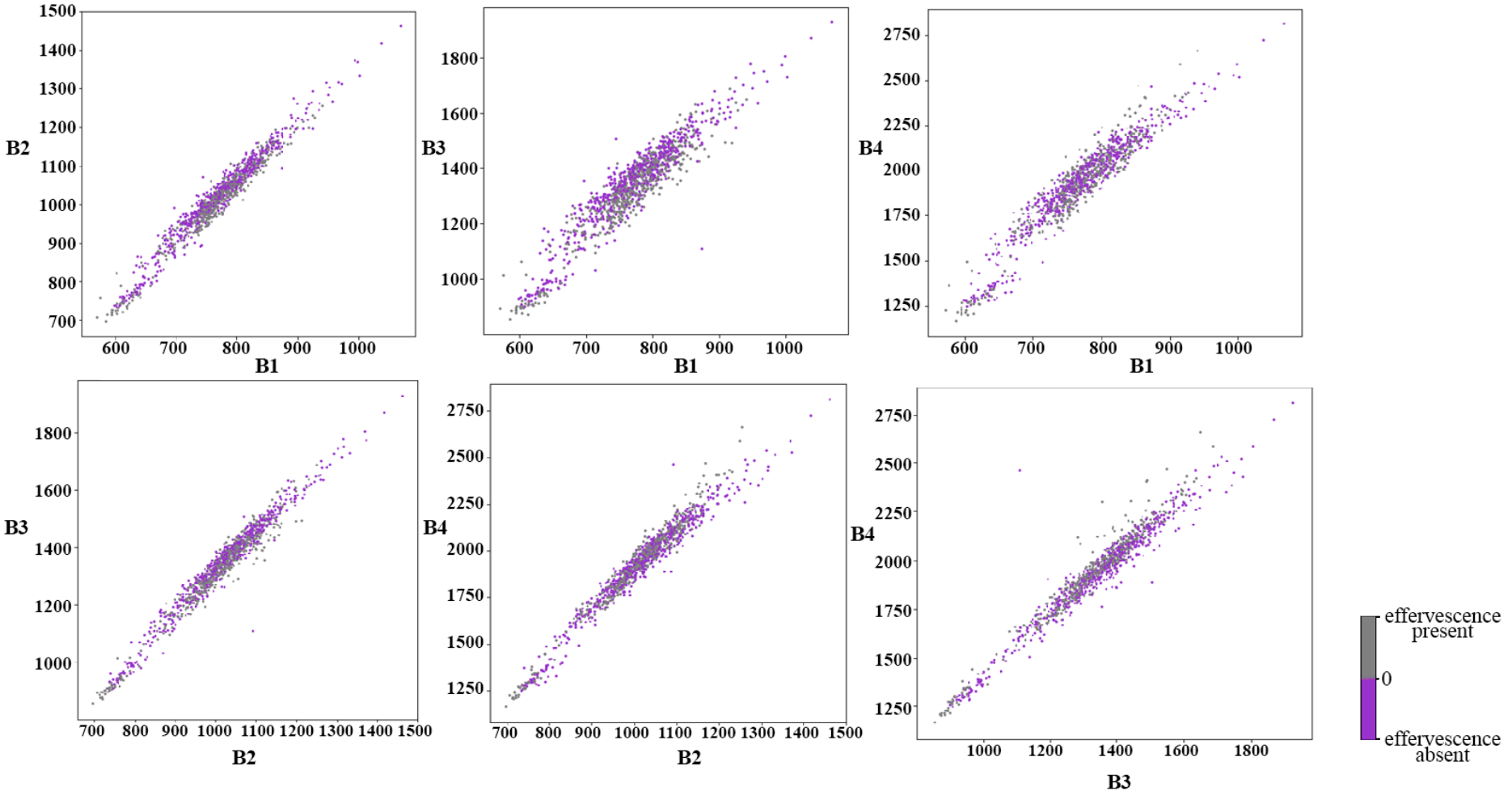

Fig. 7. Scatterplots of pixel brightness and soil effervescence (present/absent) at the sampling plots in the key area with an open soil surface, presented in the Blue (B1), Green (B2), Red (B3) and NIR (B4) channels and compiled using the Pleiades satellite image, 25/04/2020.

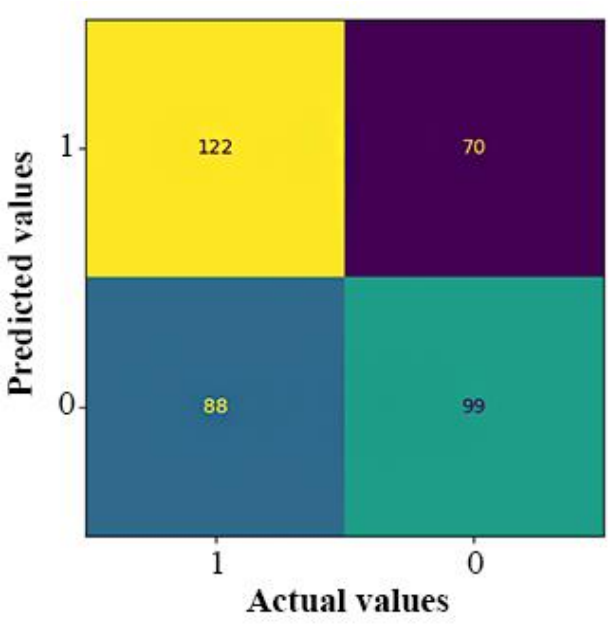

Fig. 8. Error matrix of the classified image of the key area for surface soil effervescence (present/absent) based on the Pleiades satellite image, 25/04/2020.

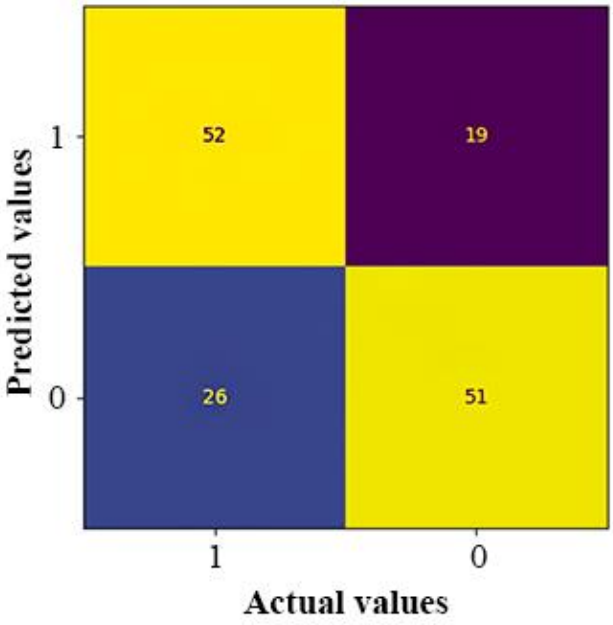

Fig. 9. Error matrix of the classified image of the key area for surface soil effervescence (strong/absent) based on the Pleiades high-resolution satellite image, 28/06/2020.

Table 3. Statistical indices of the image classification of the key area for surface soil effervescence (present/absent) basedon the Random Forest algorithm and the Pleiades satellite image, 25/04/2020.

Indices (metrics)	Precision	Recall	F-score	Sample
1 – effervescence is present	0.58	0.64	0.61	192
0 – effervescence is absent	0.59	0.53	0.56	187
Percentage of correct answers	–	–	0.58	379
Macro-averaging	0.58	0.58	0.58	379
Weighted arithmetic mean	0.58	0.58	0.58	379

Table 4. Statistical indices of the image classification of the key area for surface soil effervescence (strong/absent) based on the Random Forest algorithm and the Pleiades satellite image, 28/06/2020.

Indices (metrics)	Precision	Recall	F-score	Sample
1 – strong effervescence	0.67	0.73	0.7	71
0 – no effervescence	0.73	0.66	0.69	77
Percentage of correct answers	–	–	0.7	148
Macro-averaging	0.7	0.7	0.7	148
Weighted arithmetic mean	0.7	0.7	0.7	148

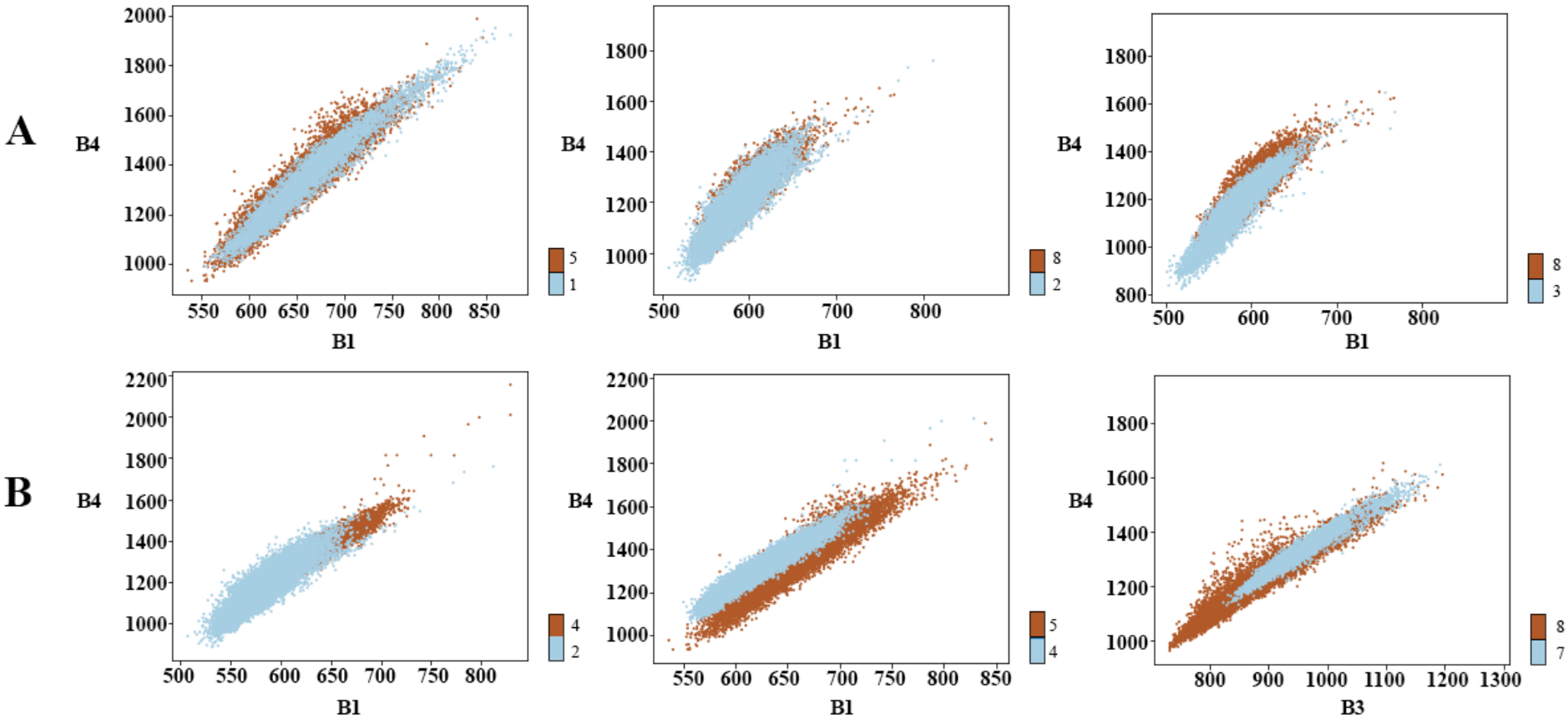

Fig. 10. Fields grouped according to their spectral brightness. *Legend:* A – similar brightness,B – different brightness, 1-8 – No. of fields.

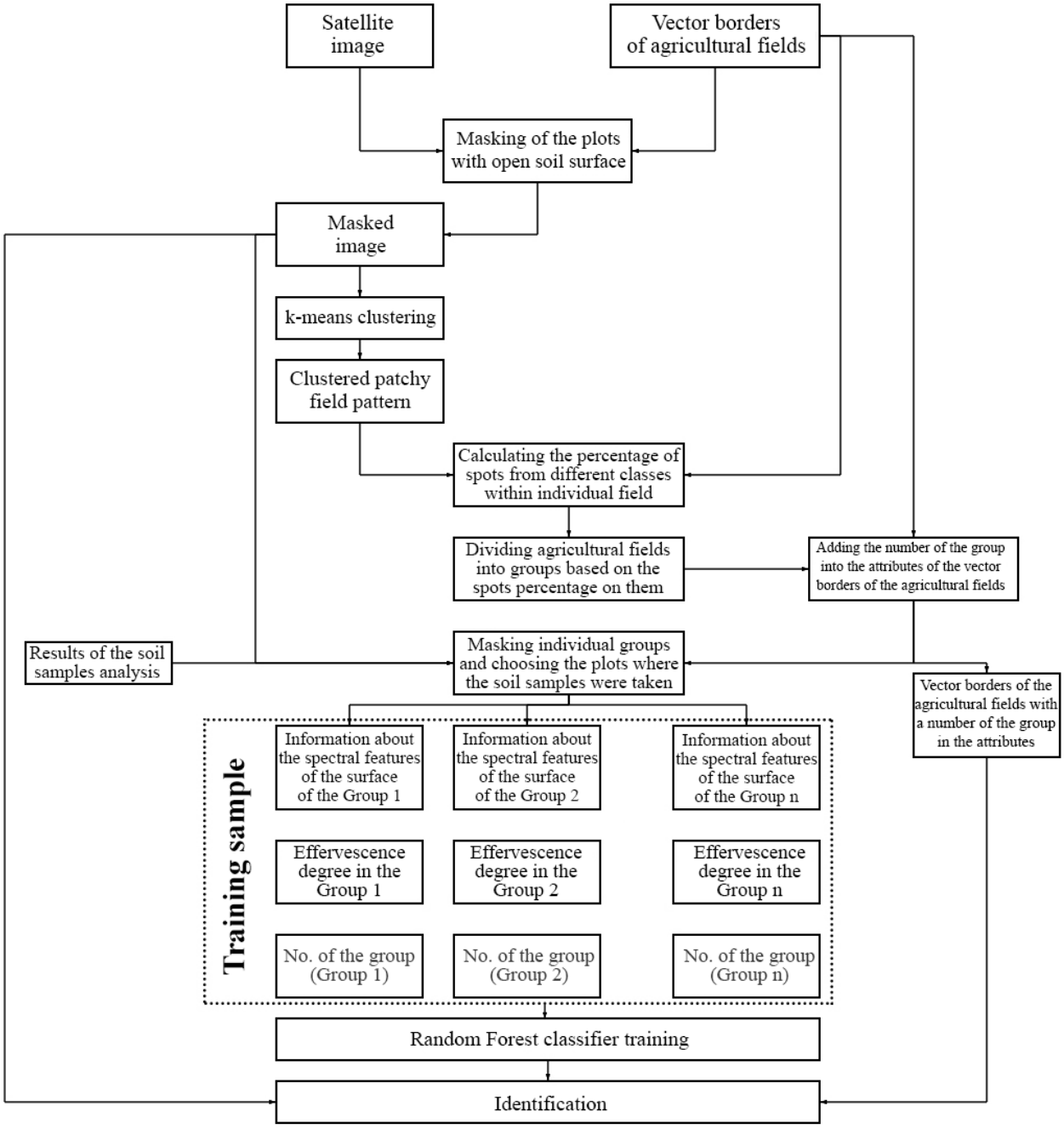

Fig. 11. Stages of auto-interpretation of a space image to classify the soils with an open surface according to their effervescence degree.

The input of the satellite image is masked to have only those fields that have an open surface and vector borders. Next, a k-means algorithm auto-clustering is used to group those fields, after which the groups of fields (or individual field) are processed individually by Random Forest, taking into account the collected field data.

Results of processing satellite images with groups of fields and individual fields. Further below we consider the results of classifying the group of fields No. 1 and 5 into 4 classes, according to the degree of their surface effervescence and using the Random Forest algorithm, where 1 is absent effervescence, 2 – weak effervescence, 3 – average, and 4 – strong. To do this we used the spectral brightness both at the sampling plots and at the additional plots around, using a sliding window

algorithm. It gave us the error matrix and statistical indices (metrics), shown in Figure 12 and Table 5. As a result of cross-validation, during which the sample was divided into 4, the classification precision was 0.881, 0.911, 0.886, and 0.928 respectively. The overall classification coefficientwas 0.91 (Table 5).

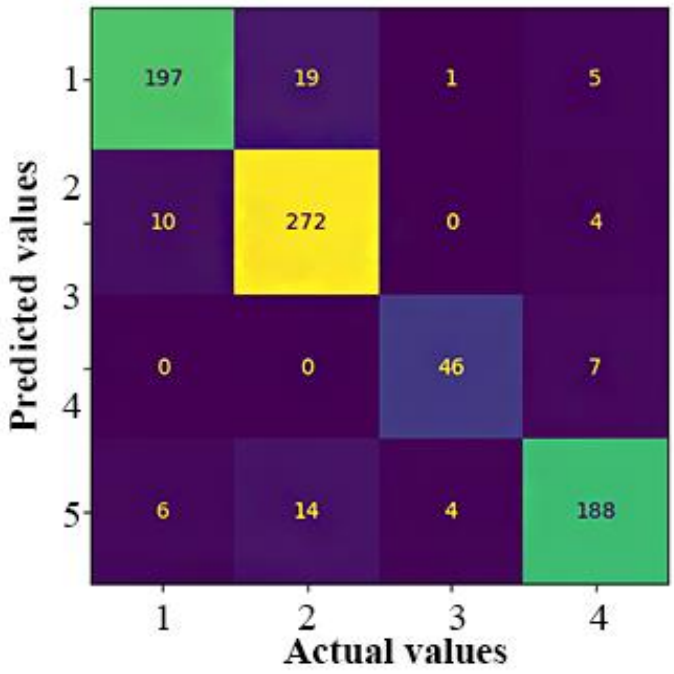

Fig. 12. Error matrix of the classified image of the fields No. 1 and 5 for their surface soil effervescence (4 classes) based on the Pleiades high-resolution satellite image, 25/04/2020.

Table 5. Statistical indices of the image classification of the fields No. 1 and 5fortheir surface soil effervescence (4 classes) based on the Random Forest algorithm and the Pleiades satellite image, 25/04/2020.

Indices (metrics)	Precision	Recall	F-score	Sample
1 – no effervescence	0.92	0.89	0.91	222
2 – weak effervescence	0.89	0.95	0.92	286
3 – average effervescence	0.90	0.87	0.88	53
4 – strong effervescence	0.92	0.89	0.90	212
Percentage of correct answers	–	–	0.91	773
Macro-averaging	0.91	0.90	0.90	773
Weighted arithmetic mean	0.91	0.91	0.91	773

Visualization of soil classification on the Pleiades satellite image, taken on 25/04/2020, was carried out according to the surface effervescence degree of the group consisting of fields No. 1, and 5 is shown in Figure 13.

After the group of fields No. 2, 3, 8 was analyzed, the classification precision was 0.54, which is not enough, and therefore, each field from this group was considered separately.

The results of statistical processing for field No. 2 that used Random Forest and spectral brightness both at sampling plots and additional plots around are presented in the error matrix and

indices (metrics) in Figure 14 and Table 6. As a result of cross-validation, during which the sample was divided into 4, the classification precision was 0.731, 0.719, 0.761, and 0.753. The overall classification coefficient was 0.75.

Visualization of soil classification on the Pleiades satellite image, taken on 25/04/2020, was carried out according to the surface effervescence of the field No. 2, and is shown in Figure 15.

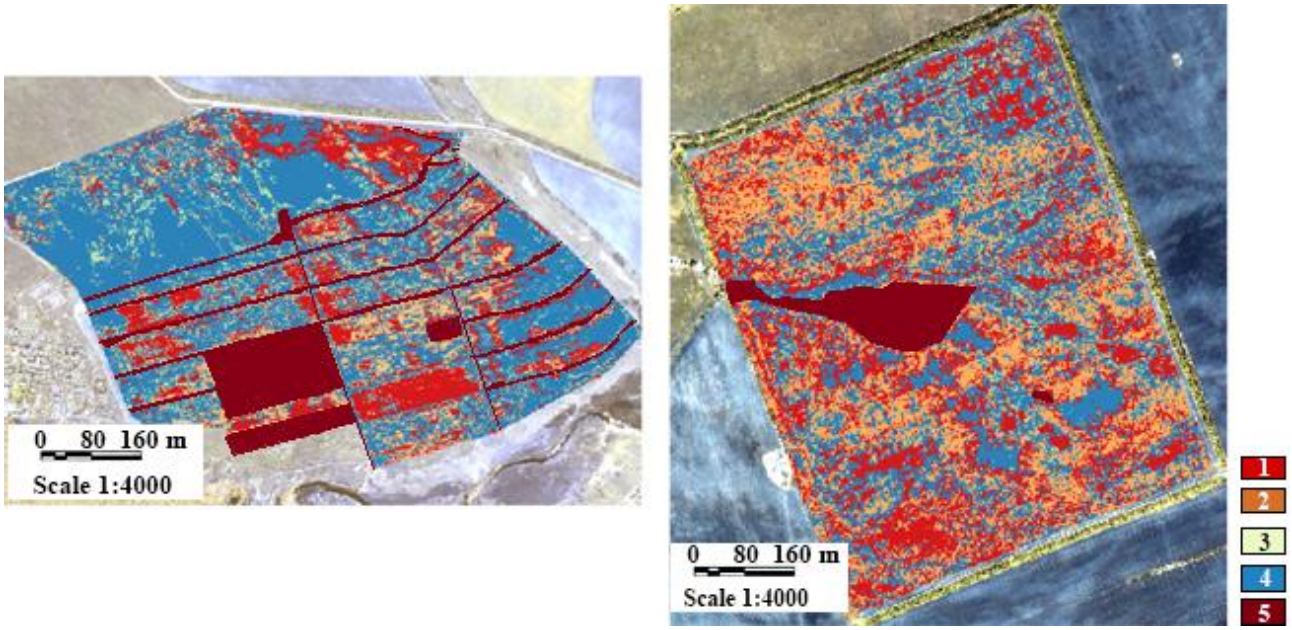

Fig. 13. Classification results for the fields No. 1 and 5, according to the degree of their surface effervescence, using the Random Forest and the Pleiades satellite image, 25/04/2020. *Legend:* 1 – no effervescence, 2 – weak effervescence, 3 –average effervescence, 4 – strong effervescence, 5 – canals, roads, hollows, parts of the fields with agricultural crops.

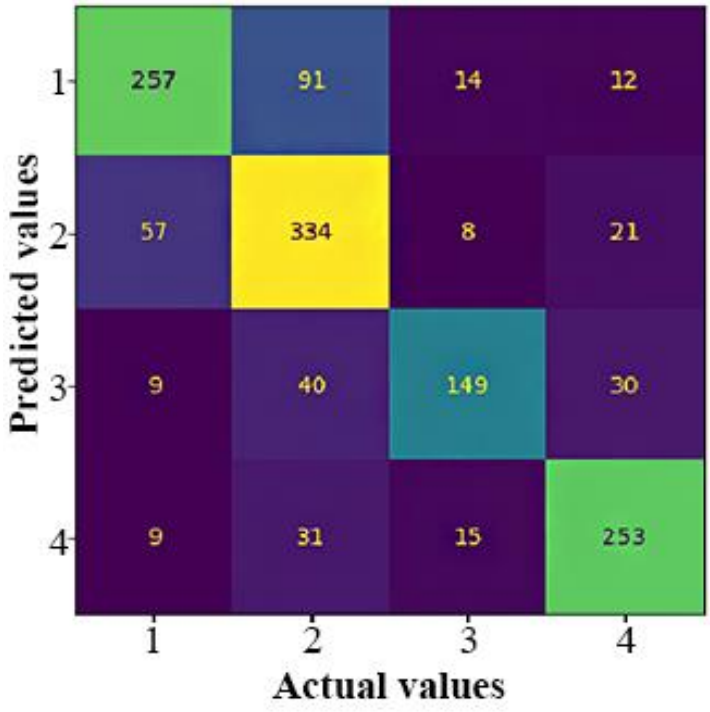

Fig. 14. Error matrix of the classified image of the field No. 2 for its surface soil effervescence (4 classes) based on the Pleiades high-resolution satellite image, 25/04/2020.

Table 6. Statistical indices of the image classification of the field No. 2 for its surface soil effervescence (4 classes) based on the Random Forest algorithm and the Pleiades satellite image, 25/04/2020.

Indices (metrics)	Precision	Recall	F-score	Sample
1 – no effervescence	0.77	0.69	0.73	374
2 – weak effervescence	0.67	0.80	0.73	420
3 – average effervescence	0.80	0.65	0.72	228
4 – strong effervescence	0.80	0.82	0.81	308
Percentage of correct answers	–	–	0.75	1330
Macro-averaging	0.76	0.74	0.75	1330
Weighted arithmetic mean	0.75	0.75	0.75	1330

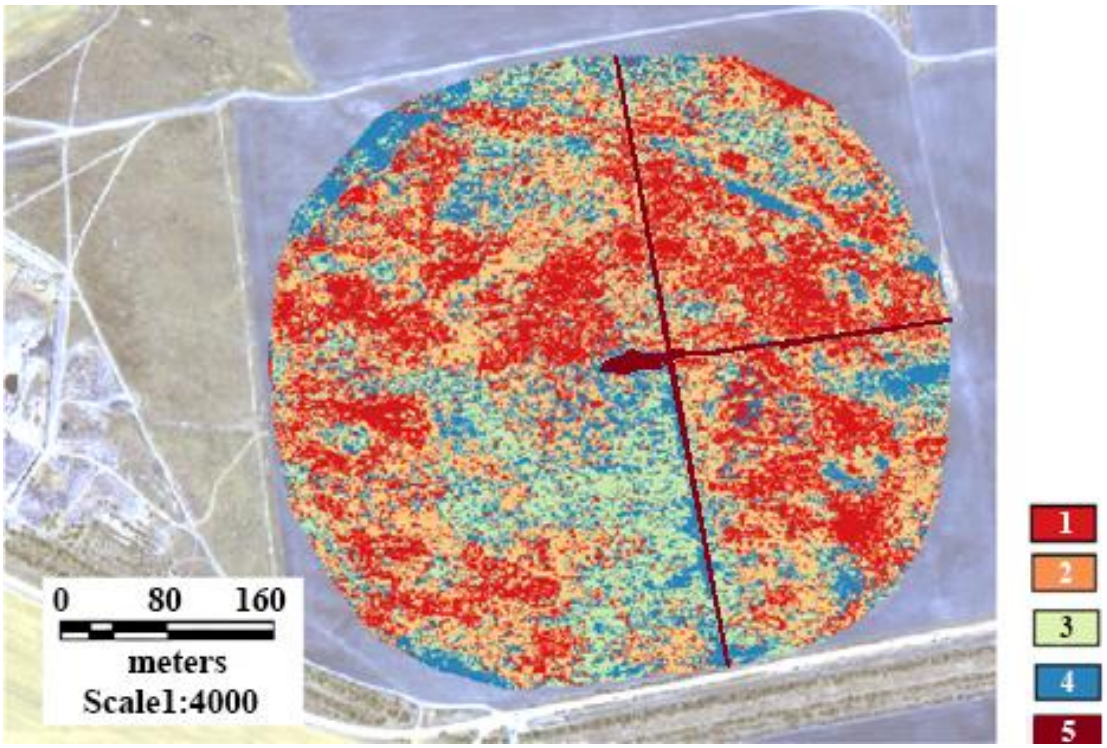

Fig. 15. Classification results for the field No. 2, according to the degree of its surface effervescence, using the Random Forest and the Pleiades satellite image, 25/04/2020. *Legend:* 1 – no effervescence, 2 – weak effervescence, 3 –average effervescence, 4 – strong effervescence, 5 – canals, roads, hollows.

The error matrix and statistical indices (metrics) for the field No. 8 are shown in Figure 16 and Table 7. As a result of cross-validation, during which the sample was divided into 4, the classification precision was 0.767, 0.769, 0.756, and 0.774. The overall classification coefficient was 0.77.

Visualization of soil classification on the Pleiades satellite image, taken on 25/04/2020, was carried out according to the surface effervescence of the field No. 8, and is shown in Figure 17.

We had the most field routes in the field No. 3 to determine the surface soil effervescence

(Fig. 2). However, it should be noted that up to 1/3 of the field was occupied by meadowish- and meadow-chestnut soils. Further below we describe the processing without excluding these soils from our sample in order to determine their influence on the classification precision.
The error matrix and indices (metrics) for the field No. 3 are shown in Figure 18 and Table 8. As a result of cross-validation, during which the sample was divided into 4, the classification precision was 0.625, 0.613, 0.608, and 0.625. The overall classification coefficient was 0.65.

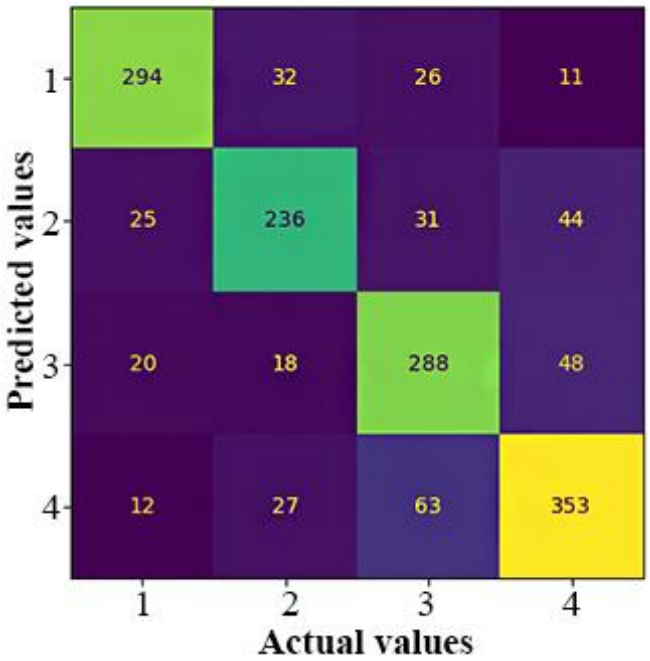

Fig. 16. Error matrix of the classified image of the field No. 8 for its surface soil effervescence (4 classes) based on the Pleiades high-resolution satellite image, 25/04/2020.

Table 7. Statistical indices of the image classification of the field No. 8 for its surface soil effervescence (4 classes) based on the Random Forest algorithm and the Pleiades satellite image, 25/04/2020.

Indices (metrics)	Precision	Recall	F-score	Sample
1 – no effervescence	0.84	0.81	0.82	363
2 – weak effervescence	0.75	0.70	0.73	336
3 – average effervescence	0.71	0.77	0.74	374
4 – strong effervescence	0.77	0.78	0.77	455
Percentage of correct answers	–	–	0.77	1528
Macro-averaging	0.77	0.76	0.77	1528
Weighted arithmetic mean	0.77	0.77	0.77	1528

The classification precision of the field No. 3 turned out to be the lowest (0.65) among all processed images, although this field had more points than others. This confirms our conclusion that meadowish- and meadow-chestnut soils, which usually are not calcareous, have effervescence and fall into the class of calcareous soils due to the fact that plowing and water bring the carbonates into them from the nearby areas. Therefore, before processing satellite data, meadowish and meadow soils should be excluded from the samples in order to prevent them from affecting the classification precision.

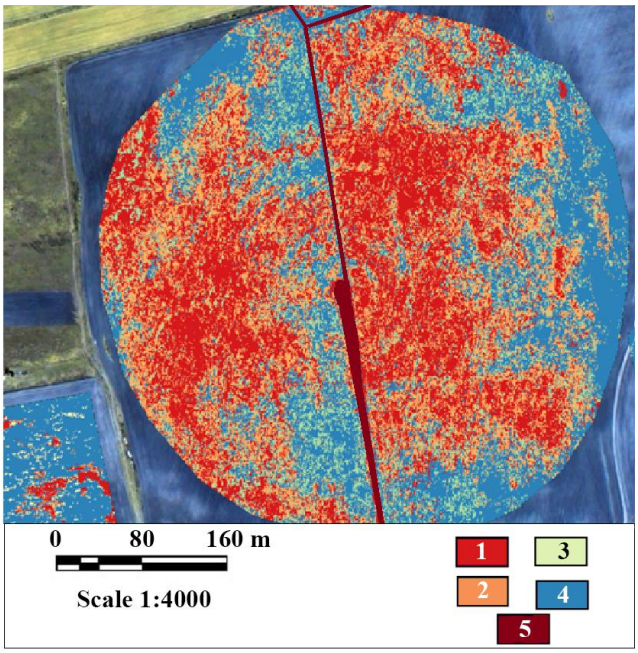

Fig. 17. Classification results for the field No. 8, according to the degree of its surface effervescence, using the Random Forest and the Pleiades satellite image, 25/04/2020. *Legend:* 1 – no effervescence, 2 – weak effervescence, 3 –average effervescence, 4 – strong effervescence, 5 – roads, traces left by irrigation structures.

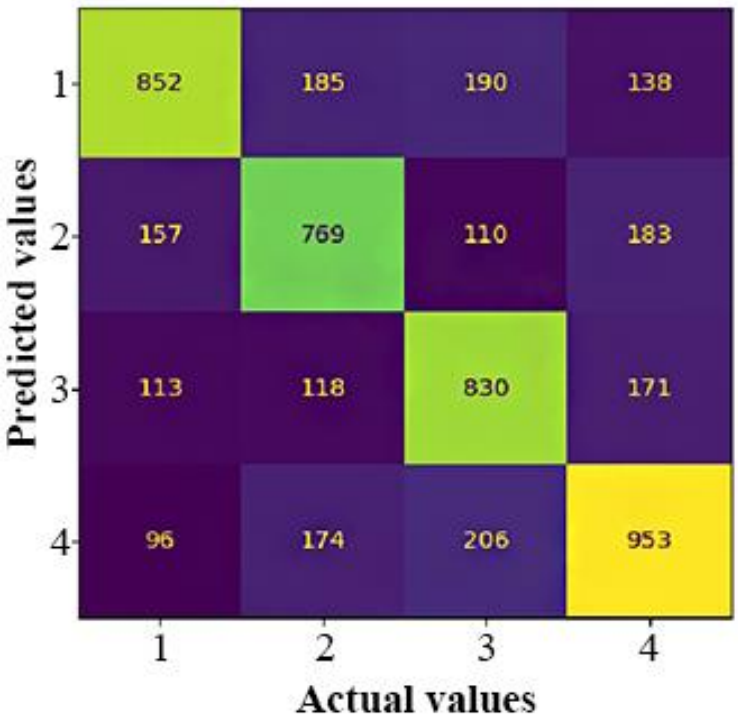

Fig. 18. Error matrix of the classified image of the field No. 3 for its surface soil effervescence (4 classes) based on the Pleiades high-resolution satellite image, 25/04/2020.

Visualization of soil classification on the Pleiades satellite image, taken on 25/04/2020, was carried out according to the surface effervescence of the field No. 3, and is shown in Figure 19.

Table 8. Statistical indices of the image classification of the field No. 3 for its surface soil effervescence (4 classes) based on the Random Forest algorithm and the Pleiades satellite image, 25/04/2020.

Indices (metrics)	Precision	Recall	F-score	Sample
1 – no effervescence	0.70	0.62	0.66	1365
2 – weak effervescence	0.62	0.63	0.62	1219
3 – average effervescence	0.62	0.67	0.65	1232
4 – strong effervescence	0.66	0.67	0.66	1429
Percentage of correct answers	–	–	0.65	5245
Macro-averaging	0.65	0.65	0.65	5245
Weighted arithmetic mean	0.65	0.65	0.65	5245

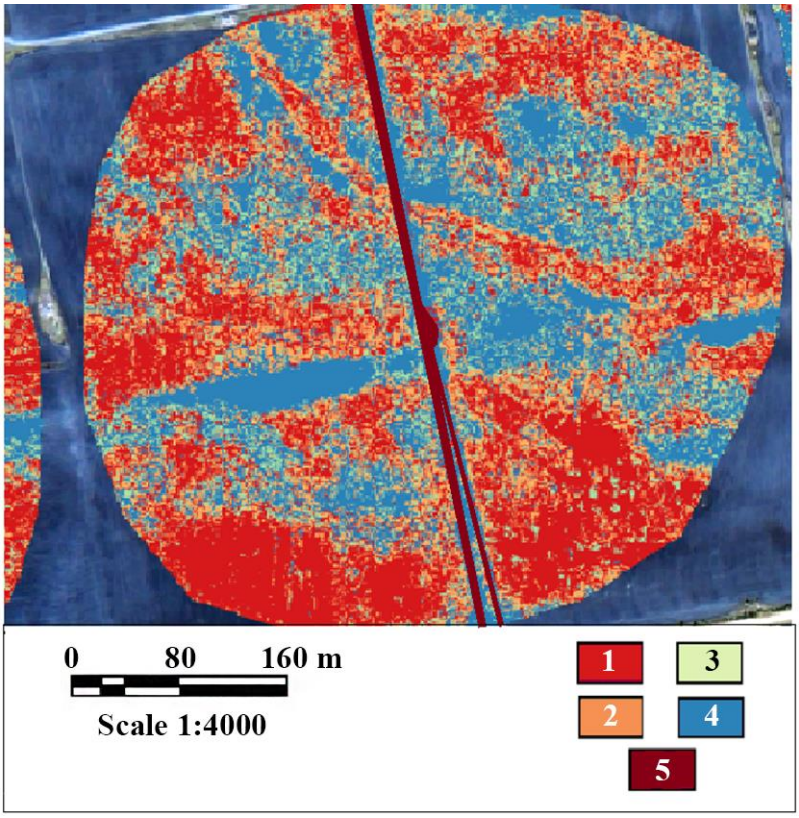

Fig. 19. Classification results for the field No.3, according to the degree of its surface effervescence, using the Random Forest and the Pleiades satellite image, 25/04/2020. *Legend:* 1 – no effervescence, 2 – weak effervescence, 3 –average effervescence, 4 – strong effervescence, 5 – roads, traces left by irrigation structures.

Conclusions

The obtained results allow us to believe that the combined use of high-resolution satellite imagery and field survey data make it possible to reliably identify calcareous surface soils, if the certain requirements of the methodology are followed, such as:

– to choose dry season (May-July) for field surveys and date when the images were taken;

– to avoid using fields with vegetating crops, fallows and those located outside of agricultural development when processing an image;

– to exclude meadowish- and meadow-chestnut soils from the sample, because humus content and soil moisture interfere with the brightness of the pixels, while the additionally introduced carbonates can corrupt the calculations.

The allocation of areas, according to their degree of soil effervescence on the open surface and using remote data is most preferable for the single fields or a group of fields that have similar brightness level. The difference in brightness on a satellite image is due to different soil moisture, as well as the type of land use, such as dry farming and irrigation. The brightness of the pixels in one image can vary even for the same type of soil of different fields. Such a differentiated approach makes the precision of soil classification based on the effervescence degree (absent, weak, average, strong) reach 0.75-0.90; while the processing of the entire area makes it possible to identify calcareous soils by effervescence only using “strong effervescence” or “absent effervescence”, bringing the precision to 0.7.

Funding. This work was carried out for the state assignments No. 0439-2022-0009 “To Study the Transformation, Evolution and Degradation of the Soil Cover in the Agricultural Landscapes at Different Levels of Organization, Including the Heterogeneity of Their Fields and Using Ground Surveys along with Digital Technologies”.

REFERENCES

1. Antipov-Karataev IN. Amelioration of solonetzes in the USSR [*Melioratsiya solontsov v SSSR*]. Moscow: Izd-vo AN SSSR, 1953:563.
2. Reservoirs, ponds and lakes of the Volgograd region [*Vodohranilishcha, prudy i ozyora Volgogradskoj oblasti*] / ed. A.S. Ovchinnikov. Volgograd: FGBOU VO Volgogradsky GAU, 2020:352.
3. Volgograd region: natural conditions, resources, economy, population, geoecological condition [*Volgogradskaya oblast’: prirodnye usloviya, resursy, hozyajstvo, naselenie, geoekologicheskoe sostoyanie*]. Volgograd: Peremena, 2011:528.
4. Vysotsky GN. Ergenia: a cultural and phytological essay [*Ergenya: kul’turno-fitologicheskij ocherk*] *Proc. of the Bureau of Applied Botany [Trudy byuro po prikladnoj botanike]*. Petrograd: Tipografiya K. Mattisena v Yur’yeve, 1915:331.
5. Gorokhova IN, Khitrov NB, Prokopyeva KO, Harlanov VA. Soil

REFERENCES

1. *Антипов-Каратаев И.Н.* 1953. Мелиорация солонцов в СССР. М.: Изд-во АН СССР. 563 с.
2. Водохранилища, пруды и озёра Волгоградской области. 2020 / Ред. А.С. Овчинников. Волгоград: ФГБОУ ВО Волгоградский ГАУ. 352 с.
3. Волгоградская область: природные условия, ресурсы, хозяйство, население, геоэкологическое состояние. 2011. Волгоград: Перемена. 528 с.
4. *Высоцкий Г.Н.* 1915. Ергеня: культурно-фитологический очерк / Труды бюро по прикладной ботанике. Петроград: Типография К. Маттисена в Юрьеве. 331 с.
5. *Горохова И.Н., Хитров Н.Б., Прокопьева К.О., Харланов В.А.* 2018. Почвенный покров Светлоярской оросительной системы через полвека мелиоративных воздействий // Почвоведение. № 8. С. 1-18. [*Gorokhova I.N., Khitrov N.B., Prokop’eva K.O., Kharlanov V.A.* 2018. Soil Cover of the Svetloyarsk Irrigation

Cover of the Svetloyarsk irrigation system after 50 years of reclamation practices. *Eurasian Soil Science.* 2018;51(8):1-11.
6. Gorokhova IN, Chursin IN, Khitrov NB, Pankova YeI. Agricultural lands identification on the satellite imagery. *Ecosystems: Ecology and Dynamics.* 2021;5(3):34-59.
7. Degtyareva ET, Zhulidova AN. Soils of the Volgograd region *[Pochvy Volgogradskoy oblasti*]. Volgograd: Nizhne-Volzhskoye knizhnoye izd-vo, 1970:319.
8. Dimo NA, Keller BA. In the semi-desert region: Soil and botanical studies in the south of Tsaritsynskyuyezd of Saratov province [*V oblasti polupustyni: Pochvennye i botanicheskie issledovaniya na yuge Caricinskogo uezda Saratovskoj gubernii*]. Saratov: Izd-vo Saratovskogo gubernskogo zemstva, 1907;3-185.
9. Zinchenko EV, Gorokhova IN, Kruglyakova NG, Khitrov NB. The current state of irrigated soils in the south of the Volga Upland [Sovremennoye sostoyaniye oroshayemykh pochv yuga Privolzhskoy vozvyshennosti] *Bulletin of the V.V. Dokuchaev Soil Institute.* 2020;104:68-109.
10. Ivanova EI. Review of the soils of the southern part of the Pre-Ural Plateau and adjacent areas of the Caspian Lowland [*Ocherk pochv yuzhnoy chasti Podural'skogo plato i prilegayushchikh rajonov Prikaspiyskoy nizmennosti*]. Leningrad: Izd-vo AN SSSR, 1928:320.
11. Ivanova EN, Friedland VM. Soil complexes of dry steppes and their evolution [*Pochvennye kompleksy suhih stepej i ih evolyuciya*] Issues of improving the food supply in the steppe, semi-desert and desert zones of the USSR [*Voprosy uluchsheniya kormovoj bazy v stepnoj, polupustynnoj i pustynnoj zonah SSSR*]. Moscow-Leningrad: Izd-vo AN SSSR, 1954:162-190.

System after 50 Years of Reclamation Practices // Eurasian Soil Science. Vol. 51. No. 8. P. 1-11.]
6. *Горохова И.Н., Чурсин И.Н., Хитров Н.Б., Панкова Е.И.* 2021. Распознавание сельскохозяйственных угодий по космическим снимкам // Экосистемы: экология и динамика. Т. 5. № 3. С. 5-33. [*Gorokhova I.N., Chursin I.N., Khitrov N.B., Pankova Ye.I.* 2021. Agricultural Lands Identification on the Satellite Imagery // Ecosystems: Ecology and Dynamics. Vol. 5. No. 3. P. 34-59.]
7. *Дегтярева Е.Т., Жулидова А.Н.* 1970. Почвы Волгоградской области. Волгоград: Нижне-Волжское книжное изд-во. 319 с.
8. *Димо Н.А., Келлер Б.А.* 1907. В области полупустыни: Почвенные и ботанические исследования на юге Царицинского уезда Саратовской губернии. Саратов: Изд-во Саратовского губернского земства. С. 3-185.
9. *Зинченко Е.В., Горохова И.Н., Круглякова Н.Г., Хитров Н.Б.* 2020. Современное состояние орошаемых почв юга Приволжской возвышенности // Бюллетень Почвенного института имени В.В. Докучаева. Вып. 104. М.: РАСХН. С. 68-109.
10. *Иванова Е.И.* 1928. Очерк почв южной части Подуральского плато и прилегающих районов Прикаспийской низменности. Л.: Изд-во АН СССР. 320 с.
11. *Иванова Е.Н., Фридланд В.М.* 1954. Почвенные комплексы сухих степей и их эволюция // Вопросы улучшения кормовой базы в степной, полупустынной и пустынной зонах СССР. М.-Л.: Изд-во АН СССР. С. 162-190.
12. Классификация и диагностика почв России. 2004. Смоленск: Ойкумена. 342 с.
13. *Роде А.А.* 1947. Почвообразовательный

12. Classification and diagnostics of soils in Russia [*Klassifikaciya i diagnostika pochv Rossii*]. Smolensk: Oikumena, 2004:342 p.
13. Rode AA. Soil formation and evolution [*Pochvoobrazovatel'nyy protsess i evolyutsiya pochv*]. Moscow: Geografgiz, 1947:142.
14. Guide to the description of soils [*Rukovodstvo po opisaniyu pochv*]. Rome: FAO, 2012:101.
15. Diagnosis and Improvement of Saline and Alkali Soils / ed. L.A. Richards. USDA. Agriculture Handbook. 1954;60:160.
16. Guidelines for Soil Description. 4th ed. Rome: FAO, 2006:98.
17. Tian F, Hou M, Qiu Y, Zhang T, Yuan Y. Salinity Stress Effects on Transpiration and Plant Growth under Different Salinity Soil Levels Based on Thermal Infrared Remote (TIR) Technique. *Geoderma.* 2020;357:113961.
18. Wang F, Shi Z, Biswas A, Yang S, Ding J. Multi-Algorithm Comparison for Predicting Soil Salinity. *Geoderma.* 2020;365: 114211.
19. Wang J, Ding J, Yu D, Ma X, Zhang Z, Ge X, Teng D, Li X, Liang J, Lizaga I, Chen X, Yuan L, Guo Y. Capability of Sentinel-2 MSI Data for Monitoring and Mapping of Soil Salinity in Dry and Wet Seasons in the Ebinur Lake Region, Xinjiang, China. *Geoderma.* 2019;353:172-187.
20. Zarea E, Arshad M, Zhao D, Nachimuthu G, Triantafilis J. Two-dimensional time-lapse imaging of soil wetting and drying cycle using EM38 data across a flood irrigation cotton field. *Agricultural Water Management.* 2020;241:106383. https://doi.org/10.1016/j.agwat.2020.106383

процесс и эволюция почв. М.: Географгиз. 142 с.
14. Руководство по описанию почв. 2012. Рим. Продовольственная и сельскохозяйственная организация объединенных наций. 101 с.
15. Diagnosis and Improvement of Saline and Alkali Soils. 1954 / Ed. L.A. Richards USDA. Agriculture Handbook. No. 60. 160 p.
16. Guidelines for Soil Description. 2006. 4th ed. Rome: FAO. 98 p.
17. *Tian F., Hou M., Qiu Y., Zhang T., Yuan Y.* 2020. Salinity Stress Effects on Transpiration and Plant Growth under Different Salinity Soil Levels Based on Thermal Infrared Remote (TIR) Technique // Geoderma. Vol. 357. P. 113961.
18. *Wang F., Shi Z., Biswas A., Yang S., Ding J.* 2020. Multi-algorithm Comparison for Predicting Soil Salinity // Geoderma. Vol. 365. P. 114211.
19. *Wang J., Ding J., Yu D., Ma X., Zhang Z., Ge X., Teng D., Li X., Liang J., Lizaga I., Chen X., Yuan L., Guo Y.* 2019. Capability of Sentinel-2 MSI Data for Monitoring and Mapping of Soil Salinity in Dry and Wet Seasons in the Ebinur Lake Region, Xinjiang, China // Geoderma. Vol. 353. P. 172-187.
20. *Zarea E., Arshad M., Zhao D., Nachimuthu G., Triantafilis J.* 2020. Two-dimensional time-lapse imaging of soil wetting and drying cycle using EM38 data across a flood irrigation cotton field // Agricultural Water Management. No. 241. P. 106383. https://doi.org/10.1016/j.agwat.2020.106383

УДК 631.4

ВЫДЕЛЕНИЕ КАРБОНАТНЫХ ПОЧВ НА ВОЛГО-ДОНСКОЙ ОРОСИТЕЛЬНОЙ СИСТЕМЕ (ВОЛГОГРАДСКАЯ ОБЛАСТЬ) С ИСПОЛЬЗОВАНИЕМ КОСМИЧЕСКОЙ ИНФОРМАЦИИ

© 2023 г. И.Н. Горохова*, И.Н. Чурсин, Н.Б. Хитров*, Н.К. Круглякова*, *****

**Почвенный институт им. В.В. Докучаева*
Россия, 119017, г. Москва, Пыжевский пер., стр. 7. E-mail: g-irina14@yandex.ru
***Научный геоинформационный центр РАН*
Россия, 119019, г. Москва, а/я 168, ул. Новый Арбат, д. 11. E-mail: chursin.ivan93@gmail.com
****Всероссийский научно-исследовательский институт орошаемого земледелия*
Россия, 400002, г. Волгоград, ул. им. Тимирязева, д. 9. E-mail: kruglyakova02032013@yandex.ru

Поступила в редакцию 16.12.2022. После доработки 01.02.2023. Принята к публикации 02.02.2023.

Исследование направлено на обоснование выделения ареалов карбонатных почв с использованием космической информации высокого разрешения (Pleiades) на территории ключевого участка опытной станции «Орошаемая» Волго-Донской оросительной системы, расположенной в Волгоградской области. Проблема с присутствием карбонатов в почвах связана с тем, что они оказывают как положительное, так и отрицательное воздействие на почвы, поэтому выявление таких почв практически важно. Выделение на космических снимках карбонатных пятен проводилось по точкам поверхностного вскипания почв разной степени от раствора HC1, которое выявлялось контактным способом на с/х полях. Далее осуществлялась установка связи между спектральной яркостью в разных каналах космического снимка в точках вскипания и степенью вскипания почв. Для этого с космических изображений делалась выборка из пикселей, соответствовавших точкам вскипания на поверхности почв на местности, которая использовалась при выделении классов на снимке с помощью алгоритма RandomForest. В результате всех проведенных исследований было определено, что для выделения ареалов карбонатных (вскипающих) с поверхности почв по космической информации оптимально проводить полевые измерения и использовать материалы съемки в засушливый сезон года (май-июль). При обработке снимка следует использовать изображение полей с открытой поверхностью почв и не вовлекать территории за пределами сельскохозяйственного освоения. Необходимо также исключать из выборки точки с луговато- и лугово-каштановыми почвами. Они расположены, как правило, в понижениях рельефа и из-за привнесенных со стороны карбонатов могут создавать помехи в расчетах. Выделение ареалов карбонатных почв лучше всего проводить в рамках отдельного с/х поля или группы схожих по яркости полей. Разброс яркости с/х полей на космическом снимке возникает из-за разного вида использования земель (богара, орошаемое поле). При таком дифференцированном подходе точность классификации карбонатных почв по степени вскипания (нет, слабое, среднее и сильное) на космическом изображении достигает 0.75-0.90, в то время как при обработке ключевого участка целиком, возможно выделение карбонатных почв только с градацией сильное вскипание или нет вскипания с точностью 0.7. Новизна результатов работы заключается в обосновании возможности достоверного выделения поверхностно-карбонатных почв при совместном использовании материалов космической информации высокого разрешения и данных полевых обследований при условии соблюдения определенных требований.

Ключевые слова: карбонатные почвы, вскипание, степень вскипания почв, открытая поверхность, космические снимки, спектральная яркость, точность классификации, Волгоградская область.

Финансирование. Работа выполнена по теме государственных заданий № 0439-2022-0009 «Изучить трансформацию, эволюцию и деградацию почвенного покрова агроландшафтов на разных уровнях организации, включая внутриполевую неоднородность с использованием сочетания наземных обследований и цифровых технологий».

DOI: 10.24412/2542-2006-2023-1-92-114

EDN: CXMSUO